

# Revisiting Impedance-based Criteria for Converter-Based AC System

Chongbin Zhao, *Student Member, IEEE*, and Qirong Jiang

**Abstract**—Multiple types of Nyquist-like impedance-based criteria are utilized for the small-signal stability analysis of converter-based AC systems. It is usually considered that the eigenvalue-based criterion can identify a critical loop apart from the overall attribute given by the determinant-based criterion. This paper specifies such understandings starting with the zero-pole calculation of impedance matrices obtained by state-spaces with the Smith-McMillan form, then clarifying the absolute reliability of determinant-based criterion with the common assumption for impedance-based analysis that each subsystem can stably operate before the interconnection. On the other hand, ambiguities exist for the eigenvalue-based criterion due to the square root of the transfer function, which takes away the intuitiveness of Nyquist plots where the open-loop right-half plane pole checks or the encirclement direction around the origin can be ignored. To this end, a logarithmic derivative-based criterion to directly identify the system modes using the frequency responses of loop impedances is proposed, which owns a solid theoretical basis of the Schur complement of transfer function matrices. The grid-connected example of a two-level voltage source converter is focused on, and simulation results in PSCAD match the theoretical analyses.

**Index Terms**—Impedance-based method, AC system, Smith-McMillan form, stability criterion, determinant, eigenvalue

## I. INTRODUCTION

LEARNING from the successful practices in DC systems since the 1970s [1], [2], the impedance-based criterion has been extended to converter-dominated AC systems for (small-signal) stability analyses in the recent ten years. It enables vendors to stabilize their design under ideal grids and the utilities to examine interconnections using frequency responses. Such advantages are acknowledged by both academic and industrial communities and lead to the relevant standards or chapters [3], [4], e.g., the impedance-ratio criterion serves as guidance for wind farm constructions in China [3], which confirms its practicability.

The so-called “impedance/admittance” refers to a transfer function that describes the small-signal ratio between voltage and current, thus the impedance-based criterion can be concluded in a Nyquist-like framework based on Cauchy’s argument principle for graphical analyses [5], [6], which is more rigorous or practical than the bode plot or the eigenvalue calculation using the state-space [7]. Since the Nyquist plots

of open-loop systems are used to identify the closed-loop stability, the *frame coupling* [8], [9] of AC rather than DC system which results in the high-dimensional open-loop transfer function matrices and the use of generalized Nyquist criterion [6] arouses broad attention. In addition, to obtain linear time-invariant systems for performing Nyquist criteria, only the linearization is sufficient for a DC system while the extra normalization to acquire the time-invariant equilibrium is required for an AC system, where the Park transformation and the harmonic balance are the two most frequently-used techniques that export the *dq* and sequence domain impedance (model), respectively [10]–[12].

By aggregating the open-loop grid- and converter-side impedance matrix considering each physical loop in the sum or ratio form [13] (i.e., the return difference or ratio), two methods can be selected for stability identification [14], [15]. The first method calculates the determinant and counts the number of encirclements of the unique locus around the origin in the Nyquist plot, which is believed to tell whether an unstable mode exists for the specific operating condition of the complete system. The second method calculates the eigenvalues of the impedance ratio, and it is reported that once a specific locus encircles the origin, the corresponding physical loop should be responsible for the instability, thus giving more physical insights. This paper will offer a group of examples to question the universality of the eigenvalue-based criterion, and it is confirmed that the unexpected right-half plane (RHP) pole leads to potential failure. Comparatively, the reliability of determinant-based criterion is explained through mathematical deduction. To sum up, an alternative is required to achieve the scope of eigenvalue-based criterion.

Obtaining the *Smith-McMillan form* [14] by diagonalization is a standard method to acquire the zeros, poles, and determinant of a transfer function matrix. Nevertheless, the approach of diagonalizing a transfer function matrix is not unique, e.g., the submatrix with Schur complement, which yields the decoupled *loop impedance* [16] that corresponds to adding a voltage perturbation in the closed-loop system, sampling the current response, and calculating the ratio. Therefore, partial system modes are reflected in the numerator while extra RHP poles may exist in the denominator, which sacrifices the aforementioned advantage of the determinant-based criterion (Note that for a one-dimensional loop impedance, the determinant- and eigenvalue-based criterion are equivalent), and using the RHP poles counting method in [17] is complicated without a direct solution on the problem since only RHP zeros are of concern.

On the other hand, if frequency responses of loop

This work was supported in part by the National Natural Science Foundation of China under Grant U22B6008. (*Corresponding author: \*\*\**).

The authors are with the Department of Electrical Engineering, Tsinghua University, Beijing 100084, China (e-mail: zhaoqb19@mails.tsinghua.edu.cn; qrijiang@mail.tsinghua.edu.cn).

> REPLACE THIS LINE WITH YOUR MANUSCRIPT ID NUMBER (DOUBLE-CLICK HERE TO EDIT) <

impedance are available, performing the vector fitting can quickly identify the zeros and poles [18], but apart from the well-known trial and error to avoid over- or under-fitting, a more critical issue is that only the specific zeros with positive real parts count for the stability analysis, which makes most of the identified results redundant, especially when a non-rational time delay is modeled in the loop impedance. A criterion to directly identify modes using frequency responses of the determinant of impedance-sum matrix is proposed in [19], which grasps the essence of this problem. The key idea in [19] is assuming a two-order polynomial of interest with a pair of conjugate roots and regarding the rest of the transfer function as a whole. By separating the real and imaginary parts of frequency responses, the concerned unstable modes with positive real parts should satisfy a specific group of conditions, but it is found in [20] that the criterion in [19] may misjudge a stable mode to be unstable. To this end, a more reliable criterion for the distributed analysis to locate the root cause of instability and complement the determinant-based overall stability analysis is necessary.

This paper aims at revisiting the origin of the impedance-based method, explicating the relative criteria, and making necessary revisions. It contributes to the following.

1) Clarifying the derivation of zeros, poles, and determinant of a transfer function matrix using the Smith-McMillan form. Particularly, the system does not contain an RHP pole when a converter can stably operate under ideal grids; the multiplication of two transfer function matrices without RHP poles surely does not introduce a new RHP pole; these are the most appealing points of impedance-based method from device-level to system-level analysis [21]-[23].

2) Perfecting a systematical method to obtain the proper zeros and poles of impedance models using the state-space in both  $dq$  and sequence domain, which guarantees the order of denominator equal to the number of system state variables and avoids the ambiguous zero-pole cancellation or emergence which are not beneficial for applying the Nyquist stability criterion.

3) Discussing the reliability of the widely used Nyquist-like determinant-based and eigenvalue-based criteria based on a comparative study. Specifically, it is recommended to avoid using the eigenvalue-based criterion because of the uncertain emergence of the RHP pole through a square root of the transfer function, and an alternative should be developed to obtain the expected physical insights of an unstable system.

4) Connecting the deduction of loop impedance with the Schur complement and the Smith-McMillan form on obtaining the system determinant. A novel criterion is then proposed based on the logarithmic derivative of frequency responses of loop impedances to directly identify the unstable modes, which equally treats each zero and pole and indicates the frequency selectivity, and its application in the system-level analysis is envisioned.

The remainder of this paper is organized as follows. Section II clarifies the theoretical foundation of impedance-based stability criteria. Section III first introduces the studied

system and derives the impedances using the state-space, then conducts the comparative studies to examine the generality of determinant- and eigenvalue-based criterion. A novel criterion to remedy the existing impedance-based criteria is proposed in Section IV. Section V discusses and concludes the work.

## II. THEORETICAL FOUNDATION

### A. Impedance Matrix of Open-loop Systems

The AC system considered in this paper is three-phase symmetrical without zero-sequence dynamics. The start of using a  $2 \times 2$   $dq$  domain transfer function matrix with non-negligible off-diagonal terms may be traced back to [10] where a constant power load is fed by an ideal AC grid. The obtained  $2 \times 2$  impedance matrix should cooperate with another  $2 \times 2$  transfer function matrix that represents the nonideal grid to perform the Nyquist-like criterion, which uses the open-loop gain to identify the closed-loop stability.

Even if modeling in the  $dq$  domain adapts to the common decoupling control and yields an inherent linear time-invariant model, an extra rotation to the public coordinate is required for the system-level analysis [11], hence the sequence domain harmonic linearization became a mainstream in recent years. The open-loop sequence domain model can be transformed from the corresponding  $dq$  domain model through a combination of rotation and frequency shift [24], and any type of (e.g.,  $\alpha\beta$ , power, and phasor domain) open-loop transfer function models [8] must be  $2 \times 2$  at the single AC terminal.

Impedance models can be directly developed in the frequency domain [25], [26] and more generically, exported from the corresponding time-domain state-space:

$$\begin{cases} \Delta \dot{\mathbf{x}} = \mathbf{A}\Delta \mathbf{x} + \mathbf{B}\Delta \mathbf{u} \\ \Delta \mathbf{y} = \mathbf{C}\Delta \mathbf{x} + \mathbf{D}\Delta \mathbf{u} \end{cases} \quad (1)$$

$$\Delta \mathbf{u}(s) = \underbrace{[\mathbf{C}(s\mathbf{I} - \mathbf{A})^{-1}\mathbf{B} + \mathbf{D}]}_{\text{Transfer Function Matrix}} \Delta \mathbf{y}(s) \quad (2)$$

where  $\mathbf{A}$ ,  $\mathbf{B}$ ,  $\mathbf{C}$ ,  $\mathbf{D}$ , and  $\mathbf{I}$  are the constant-value state, input, output, feedforward, and identity matrices, respectively.  $\mathbf{x}$ ,  $\mathbf{y}$ , and  $\mathbf{u}$  are the state, input, and output vectors formed by the corresponding variables, respectively. The prefix  $\Delta$  represents the small-signals while  $s$  is the Laplace operator.

An indication from [12] is that when the voltage source converter (VSC) serves as an open-loop current-source subsystem and accesses a voltage-source subsystem, the admittance matrix of VSC should be first established and applied for the closed-loop stability criterion. From the mathematical perspective, such a preference can be explained as the AC current dynamics are undoubtedly the elements of  $\Delta \mathbf{x}$  and  $\Delta \mathbf{y}$  while the AC voltage dynamics cannot be included in  $\Delta \mathbf{y}$ , so the transfer function matrix in (2) is the admittance matrix and the impedance matrix is the inversion of admittance matrix. In addition, all the elements in the VSC admittance (not the impedance) model should hold the same denominator that is factored by the system modes (indicated by  $(s\mathbf{I} - \mathbf{A})^{-1}$ ). Since the eigenvalues of  $\mathbf{A}$  reflects the system modes, a stable open-loop subsystem without unstable mode surely does not induce an RHP pole of each element in the



> REPLACE THIS LINE WITH YOUR MANUSCRIPT ID NUMBER (DOUBLE-CLICK HERE TO EDIT) <

$$\begin{aligned} S_Z^1 &= \Delta u^1 / \Delta i^1 = Z_g^{11} + Z_c^{11} - (Z_g^{12} + Z_c^{12})(Z_g^{21} + Z_c^{21}) / (Z_g^{22} + Z_c^{22}), \\ S_Z^2 &= \Delta u^2 / \Delta i^2 = Z_g^{22} + Z_c^{22} - (Z_g^{12} + Z_c^{12})(Z_g^{21} + Z_c^{21}) / (Z_g^{11} + Z_c^{11}), \quad (10) \\ S_V^{1/2} &= -\Delta i^{1/2} / \Delta u^{1/2} = (S_Z^{1/2})^{-1}. \end{aligned}$$

A critical observation is that the numerators of all types of Schur complements using (9) are equal to those of the determinants in (5) and (6), but the feature of RHP poles for each Schur complement is no more similar with that of  $\det(\mathbf{I} + \mathbf{RZ}_Y)$ . Hence, Nyquist-like criteria are not suitable to be performed on the Schur complements, including the idea in [16] which decomposes  $S_Z^{1/2}$  to the equivalent grid- and converter-side impedances considering the frame coupling. Taking frame “1” as an example:

$$\begin{aligned} \Delta u^1 &= \Delta u_c^1 - \Delta u_g^1 \Rightarrow \\ Z_c^1 &= -\Delta u_c^1 / \Delta i^1 = Z_c^{11} - Z_c^{12}(Z_g^{21} + Z_c^{21}) / (Z_g^{22} + Z_c^{22}), \\ Z_g^1 &= \Delta u_g^1 / \Delta i^1 = Z_g^{11} - Z_g^{12}(Z_g^{21} + Z_c^{21}) / (Z_g^{22} + Z_c^{22}), \quad (11) \\ R_{ZY}^1 &= Z_g^1 / Z_c^1, \quad S_Z^1 = Z_c^1 + Z_g^1. \end{aligned}$$

Such an idea has been prevailing since it was proposed. In the standard [3], the open-loop impedance matrices are first field-tested and transformed based on (10) and (11) for stability analyses, and the results are used to determine whether the positive- or negative-sequence circuit is responsible for the instability. However, RHP pole inspections must be done before plotting the characteristic loci even if both subsystems can stably operate under ideal grids, and the valuable application of loop impedance requires a deeper investigation.

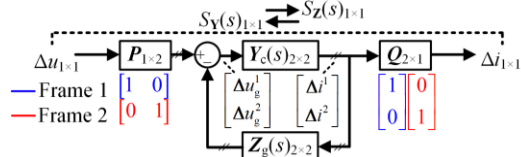


**Fig. 1.** A generalized representation of the closed-loop system to obtain the loop impedance/admittance.

### III. VALIDATION OF EXISTING IMPEDANCE-BASED CRITERIA

#### A. System Overview

With the theoretical specification in Section II, the basic scenario that a three-phase two-level VSC (TL-VSC) connects to an AC weak grid is focused on in this paper. Only the inner loop control and the phase-locked loop (PLL) are considered in the grid-following control of Fig. 2, which is simple but suits this work because:

- PLL is a decisive cause of sequence-domain frequency coupling for the converter-side impedance and admittance.
- By counting the integral outputs, AC inductor currents, and DC capacitor voltage, the system order is 8, which is quite low and benefits the zero/pole calculation.
- The obtained AC impedances are *fully observable* to the complete modes of the closed-loop system and can analyze arbitrary operating conditions.

By connecting the similarities of harmonic signal graphs between each kind of nonlinear time-periodic system [27], [28], the conclusions of a TL-VSC can be reasonably extended to other types of converters, such as the modular multilevel

converter. In addition, adopting the average model instead of the switching model in the simulation excludes the influence of PWM on stability analyses. Table I lists the key parameters for comparative studies. One can combine Fig. 2 and Table I to understand the symbol meanings.

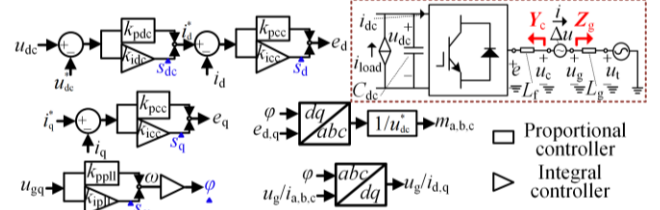


**Fig. 2.** Control loops. Superscript \* represents reference.

TABLE I  
KEY PARAMETERS OF SYSTEM

| Symbols                 | Case A   | Case B                     |
|-------------------------|--|----------------------------|
| $u_t, u_c, \omega_0$    | 380 $\angle 0^\circ$ V, 750 V, $2\pi 50$ rad/s |                            |
| $L_f, L_g, C_{dc}$      | 0.55 mH, 0.8/0.9/1.0 mH, 5 mF                  | 5 mH, 2.1/2.2/2.3 mH, 5 mF |
| $i_{load}$              | 66.66 A  | 3.1 A                      |
| $i_a$                   | 0 A  | 5 A                        |
| $k_{pdc} + k_{idc}/s$   | 0.1 + 100/s                                    | 1 + 100/s                  |
| $k_{pcc} + k_{icc}/s$   | 0.1 + 10/s                                     | 1 + 1000/s                 |
| $k_{ppll} + k_{ipll}/s$ | 3 + 100/s                                      | 5 + 2000/s                 |

#### B. Impedance Modeling Using State-space

Explicit expressions of impedance models are available using the frequency-domain operations of harmonic transfer functions for TL-VSCs but some zeros and poles are inherently “hidden” [25], [26] due to the zero-pole cancellation. Hence, a systematic approach following (1) and (2) to obtain the admittance matrix or loop admittance both in the  $dq$  and sequence domain using the state-space, is explicated in this subsection, and the system mode by calculating the eigenvalues of  $A$  can also be calculated to serve as a standard for the impedance-based analysis. Here the complete process is not offered for simplicity but some notes are added to get high-fidelity models.

- Most state-spaces are established in the  $dq$  domain for a TL-VSC, which is also the starting point of this work. Considering that the partial state variables appear in pairs (e.g.  $[s_d, s_q]$  in Fig. 1) are aligned to the *control*  $dq$  frame while the input and output of the impedance model are aligned to the *system*  $dq$  frame, the small-signal frame rotation should be included in the impedance modeling but the system modes will not be affected by the rotation.
- The rigorous equilibrium calculation by numerical iteration is the basis of linearization for any device under closed-loop control [20]. Note that there are minute changes in the state equations regarding the AC voltage dynamics between state-spaces for obtaining the open-loop impedance matrix and loop impedance, the equilibria should be kept the same based on the closed-loop system.
- The derivation of sequence domain impedance models is recommended to integrate the frame transformation from a  $dq$  domain real vector to a sequence domain complex vector into the matrices and the following (2) [29]:

> REPLACE THIS LINE WITH YOUR MANUSCRIPT ID NUMBER (DOUBLE-CLICK HERE TO EDIT) <

$$\begin{aligned} A_{pn} &= T_x^{-1}(A_{dq} + j\omega_0 I)T_x, B_{pn} = T_x^{-1}B_{dq}T_u, \\ C_{pn} &= T_y^{-1}C_{dq}T_x, D_{pn} = T_y^{-1}D_{dq}T_u. \end{aligned} \quad (12)$$

where the subscript dq/pn represents the  $dq$ /sequence domain.  $T$  represents the rotation, whose order is indicated by the subscript vectors and owns several submatrices  $0.5 \times [1, 1; -j, j]$  regarding the  $dq$  pairs.  $j$  is the imaginary unit,  $\omega_0$  is the rated angular frequency, and  $j\omega_0 I$  represents the frequency shift.

It should be noted that even if multiplying a matrix  $0.5 \times [1, 1; -j, j]$  with the variable substitution  $s$  to  $(s-j\omega_0)$  for the  $dq$  domain impedance matrix can also yield the sequence domain impedance matrix [24], the obtained transfer functions suffer the dimension explosion and using MATLAB command *mineral* to obtain the authentic zeros and poles requires trial and error. The proposed impedance derivation using state space fully avoids such an issue except in the case shown in (11), since the one-dimensional equivalent grid-/converter-side impedance is a virtual concept and does not correspond to an actual system as well as a specific state-space.

### C. Non-RHP Pole Check with Simulation Results

Fig. 3 presents the distributions of system modes for both cases in Table I when the TL-VSC accesses to ideal AC grid in the  $dq$  domain, where the grid inductor variation leads to the various operating conditions and modes. No negative damping mode is observed, i.e., no RHP pole exists for the primary output transfer functions (matrices) of the open-loop system, which indicates that both cases can be used for the stability analysis of subsystem interconnections.

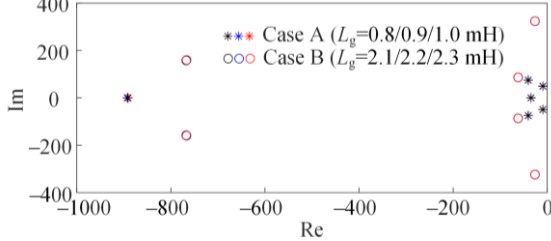


Fig. 3. Distributions of system modes.

The time-domain simulation is performed in PSCAD as Fig. 4 shows, where only the waveforms of  $u_{dc}$  are presented for their representativeness. The closed-loop system becomes unstable only if the  $L_g$  steps to the maximum setting values for both cases. Such phenomena conform to the cognition that the system tends to be unstable due to the multiple interaction patterns between the PLL and weak grid [30].

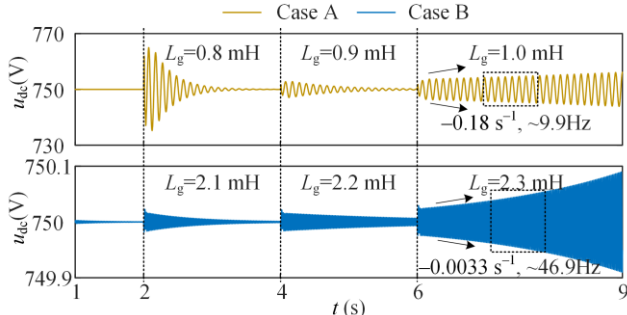


Fig. 4. Simulation waveforms of subsystem interconnections.

### D. Comparative Study on Impedance-based Criteria for Distributed Stability Analysis

This subsection will reveal the ambiguity of impedance-based criteria for distributed stability analysis, where the root cause of instability is expected to be identified. Since the generality of a criterion should be regardless of modeling frames, both the sequence and  $dq$  domain impedances are applied with discernible differences found for the two cases.

Fig. 5 illustrates the Nyquist plots of Case A. Thereinafter “1-d” represents the characteristic loci of  $RzY$  given by (11) (equals to  $\det(RzY)$ ), while “2-d” represents the characteristic loci of  $RzY$  given by (4). Because of the mutual conjugate symmetry about  $j\omega_0$  for sequence impedances and the self-symmetry about 0 for  $dq$  impedances, only one locus is shown for each sequence domain plot from  $-50$  to  $150$  Hz for simplicity, while two loci distinguished by the solid and dotted line are shown for each  $dq$  domain plot from  $-100$  to  $100$  Hz. In addition, for the number of encirclements around the origin  $(-1, j0)$ , it is different for each locus in 1-d plots, but the total encirclement should be counted for 2-d plots especially doubling the number for the sequence domain plot.

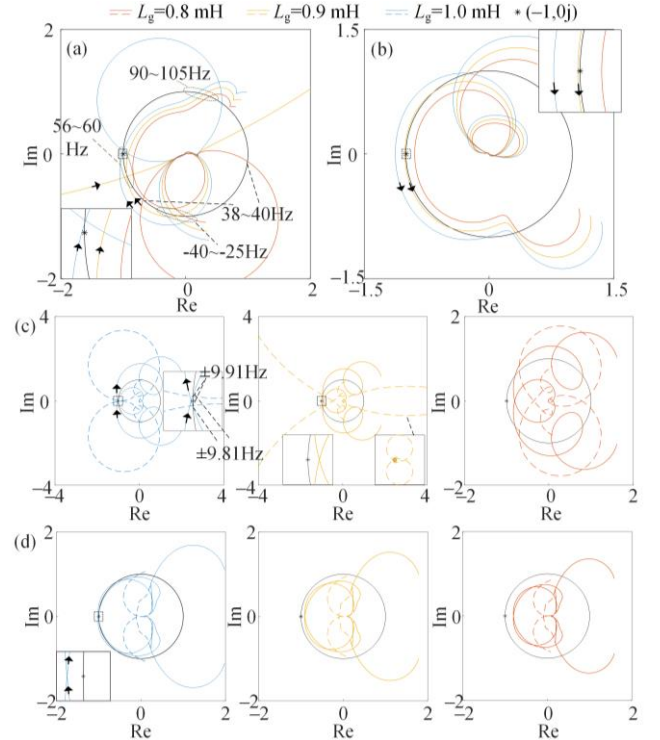


Fig. 5. Nyquist plots for Case A. (a)-(b) 1-d and 2-d in sequence domain. (c)-(d) 1-d and 2-d in  $dq$  domain.

Recalling that only setting  $L_g = 1.0$  mH can lead the system to be unstable in Fig. 4, the particularity of Case A is discussed below:

- Regarding the sequence domain 1-d plot in Fig. 5 (a), there is one clockwise encirclement when  $L_g = 1.0$  mH but one counterclockwise encirclement when  $L_g = 0.9$  mH. Whereas it can be concluded that the system is unstable when  $L_g = 1.0$  mH, it cannot be concluded that the system is stable at  $L_g = 0.9$  mH other than by inspecting the RHP

> REPLACE THIS LINE WITH YOUR MANUSCRIPT ID NUMBER (DOUBLE-CLICK HERE TO EDIT) <

poles of  $R_{ZY}$  (equals to that of  $1+R_{ZY}$ ), which can be reflected by Table II. It is observed that one RHP pole exists when  $L_g=1.0$  and  $0.9$  mH while two RHP zeros exist when  $L_g=1.0$  mH, which confirms the uncertainty of open-loop RHP pole induced by the Schur complement-based matrix diagonalization (there is no RHP pole when  $L_g=0.8$  mH) and explains the difference between locus, and because of the conjugate symmetry, there is no reason to determine whether the positive or negative sequence loop induces the instability from the Nyquist plots, i.e, the distributed stability analysis does not hold.

TABLE II  
Zeros and Poles of  $1+R_{ZY}$  ( $\times 10^2$ , Case 1)

|              |           |                              |              |                            |                              |              |
|--------------|-----------|------------------------------|--------------|----------------------------|------------------------------|--------------|
| $L_g=1.0$ mH | $Z, d, q$ | <b>0.0018</b> ±j <b>0.62</b> | -0.61 ±j4.07 | -0.27 ±j0.48               | -0.35                        | -2.26        |
|              | $P, d$    | -1.02 ±j4.72                 | -0.38 ±j0.93 | -0.10 ±j0.49               | -0.35                        | -2.19        |
|              | $q$       | -0.94 ±j3.77                 | -0.30 ±j0.44 | <b>0.10</b> ±j <b>0.58</b> | -0.35                        | -8.91        |
|              | $Z, p, n$ | <b>0.0018</b> ±j <b>3.76</b> | -0.61 ±j7.21 | -0.27 ±j3.62               | -0.35 ±j3.14                 | -2.26 ±j3.14 |
|              | $n$       | <b>0.0018</b> ±j <b>2.52</b> | -0.61 ±j0.93 | -0.27 ±j2.67               |                              |              |
|              | $H, p$    | -5.29 ±j3.12                 | -0.55 ±j7.18 | -1.72 ±j1.02               | -0.41 ±j3.76                 |              |
| $L_g=0.9$ mH | $P, p$    | -0.068 ±j3.63                | -0.35 ±j3.13 | -0.28 ±j2.67               | <b>0.024</b> ±j <b>2.48</b>  |              |
|              | $n$       | -5.29 ±j3.17                 | -0.55 ±j0.90 | -1.72 ±j7.31               | -0.41 ±j2.52                 |              |
|              | $n$       | -0.068 ±j2.65                | -0.35 ±j3.15 | -0.28 ±j3.61               | <b>0.024</b> ±j <b>3.80</b>  |              |
|              | $Z, d, q$ | -0.015 ±j0.62                | -0.66 ±j4.10 | -0.27 ±j0.49               | -0.35                        | -2.46        |
|              | $P, d$    | -1.05 ±j4.73                 | -0.40 ±j0.91 | -0.10 ±j0.49               | -0.35                        | -2.41        |
|              | $q$       | -0.95 ±j3.81                 | -0.30 ±j0.45 | 0.002 ±j0.58               | -0.35                        | -8.92        |
| $L_g=0.8$ mH | $Z, p, n$ | -0.015 ±j3.76                | -0.66 ±j0.96 | -0.27 ±j3.63               | -0.35 ±j3.14                 | -2.46 ±j3.14 |
|              | $n$       | -0.015 ±j2.52                | -0.66 ±j7.24 | -0.27 ±j2.65               |                              |              |
|              | $H, p$    | -5.43 ±j3.10                 | -0.58 ±j7.22 | -1.69 ±j1.03               | -0.41 ±j3.77                 |              |
|              | $P, p$    | -0.068 ±j3.63                | -0.35 ±j3.13 | -0.27 ±j2.66               | <b>0.0020</b> ±j <b>2.48</b> |              |
|              | $n$       | -5.43 ±j3.19                 | -0.58 ±j0.94 | -1.69 ±j7.32               | -0.41 ±j2.51                 |              |
|              | $n$       | -0.068 ±j2.65                | -0.35 ±j3.15 | -0.27 ±j3.62               | <b>0.0020</b> ±j <b>3.80</b> |              |
| $L_g=0.8$ mH | $Z, d, q$ | -0.033 ±j0.62                | -0.71 ±j4.13 | -0.27 ±j0.51               | -0.35                        | -2.70        |
|              | $P, d$    | -1.05 ±j4.73                 | -0.40 ±j0.91 | -0.10 ±j0.49               | -0.35                        | -2.41        |
|              | $q$       | -0.95 ±j3.81                 | -0.30 ±j0.45 | 0.002 ±j0.58               | -0.35                        | -8.92        |
|              | $Z, p, n$ | -0.033 ±j3.76                | -0.71 ±j7.26 | -0.27 ±j2.64               | -0.35 ±j3.14                 | -2.70 ±j3.14 |
|              | $n$       | -0.033 ±j2.53                | -0.71 ±j0.98 | -0.27 ±j3.65               |                              |              |
|              | $H, p$    | -5.60 ±j3.10                 | -0.62 ±j7.26 | -1.65 ±j1.05               | -0.41 ±j3.78                 |              |
| $L_g=0.8$ mH | $P, p$    | -0.071 ±j3.63                | -0.35 ±j3.13 | -0.26 ±j2.64               | -0.022 ±j2.48                |              |
|              | $n$       | -5.60 ±j3.20                 | -0.58 ±j0.98 | -1.69 ±j7.33               | -0.41 ±j2.50                 |              |
|              | $n$       | -0.071 ±j2.65                | -0.35 ±j3.15 | -0.26 ±j3.65               | -0.022 ±j3.80                |              |
|              | $n$       |                              |              |                            |                              |              |

Note: Z/P represents the zero/pole while  $d/p$  and  $q/n$  correspond to frames 1 and 2 in the  $dq$ /sequence domain models, respectively.

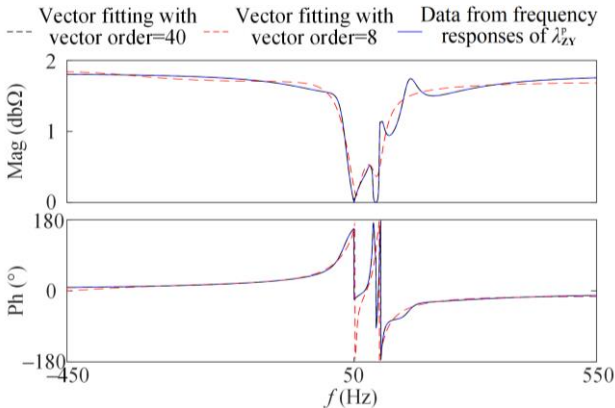


Fig. 6. Vector fitting of  $\lambda_{ZY}^p$  when  $L_g=1.0$  mH.

very confusing to use it for stability analysis because the nature of the loci does not change when  $L_g$  decreases from 1.0 mH to 0.9 mH, where two anticlockwise encirclements are both reflected and the instability when  $L_g=1.0$  mH cannot be ascertained. Even if zeros and poles of  $R_{ZY}$  can be theoretically determined by identifying each transfer function using vector fitting [18] and following Section II. B to obtain the Smith McMillan form, the implementation is complicated due to the transfer function square root in (8). For example, when setting the fitting order equals to the theoretical order  $D_{gc}$  (that is 8 in this work), the fitting error is unacceptable in Fig. 6. Only by increasing the fitting order to more than 40, it is acceptable but the numbers of identified RHP zeros and poles are questionable.

- Regarding the  $dq$  domain analysis, Fig. 5 (c) shows that for the 1-d Nyquist plot, when  $L_g=1.0$  mH, there are two clockwise encirclements around the origin for the  $d$ -locus (the solid line) instead of the  $q$ -locus (the dotted line). One may infer that the  $d$ -frame control leads to the instability, but it is not rigorous because Table II shows that  $(1+R_{ZY}^2)$  has two zeros and two poles, and no single encirclement just manifests the system to be unstable, which indicates the importance of determining the RHP poles when using the Schur complement-based criterion. While for the 2-d Nyquist plots in Fig. 5 (d), the change of loci with the variation of  $L_g$  distinguishes from Fig. 5 (b), which satisfy the expected implementation of graphical stability analyses.
- The preference of selecting a certain intersection point between the loci and unit cycle as the unstable mode may not work for Case A, especially for the sequence domain plot in Fig. 5 (a), because none of the frequencies of intersection points correspond to the simulated ( $50 \pm 9.9$ ) Hz of AC waveforms as Fig. 4 indicates, and the obtained phase margins for the same operating condition between various criteria are not consistent. Thus, it may be questionable for the quantitative information like phase margin given by the existing Nyquist-like criteria apart from judging whether or not the system is stable.

To test whether the above findings are general, Case B is well-studied with a similar process to Case A. On the whole, it is intuitive for each criterion to identify the stability using Fig. 7 even without the simpler zero-pole distribution listed in Table III, except the 2-d plot in Fig. 7 (b) since the anticlockwise encirclement around the origin for the 1-d plots are observed, but the feature of loci changes when  $L_g$  decreases from 2.3mH to 2.2mH, which differs from that in Fig. 5 (b). To sum up, even if Case B matches the existing usage of impedance-based criteria such as in [16], it cannot cover the special Case A, and only by combining the RHP pole check with the clockwise & anticlockwise identification can ensure creditable distributed stability analyses, which deviates from the origin of impedance-based analysis.

- Regarding the sequence domain 2-d plot in Fig. 5 (b), it is

> REPLACE THIS LINE WITH YOUR MANUSCRIPT ID NUMBER (DOUBLE-CLICK HERE TO EDIT) <

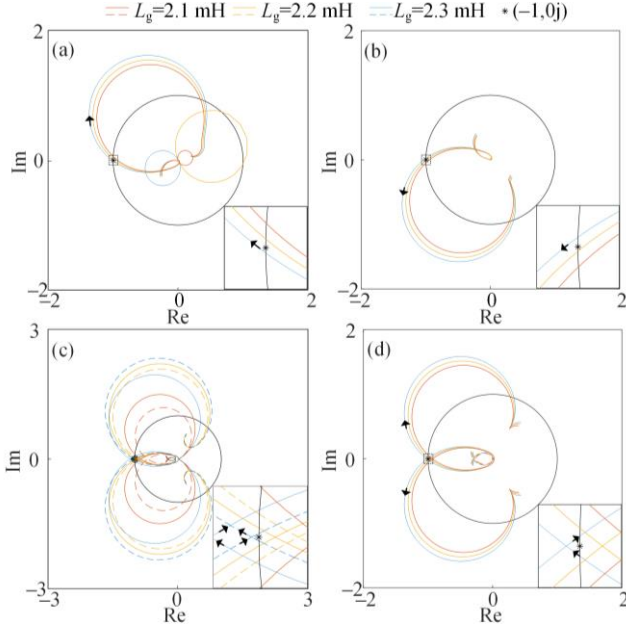


**Fig. 7.** Nyquist plots for Case B. (a)-(b) 1-d and 2-d in sequence domain. (c)-(d) 1-d and 2-d in  $dq$  domain.

**TABLE III**  
Zeros and Poles OF  $1+R_{ZY}$  ( $\times 10^2$ , Case 2)

|              |     |        |                     |                     |                    |                     |                   |
|--------------|-----|--------|---------------------|---------------------|--------------------|---------------------|-------------------|
| $L_g=2.3$ mH | $Z$ | $d, q$ | $0.0033 \pm j2.94$  | $-0.63 \pm j0.84$   | $-0.79 \pm j6.18$  | $-5.24 \pm j3.35$   |                   |
|              | $P$ | $d$    | $-0.90 \pm j6.48$   | $-5.23 \pm j3.35$   | $-0.22 \pm j3.35$  | $-0.62 \pm j0.86$   |                   |
|              |     | $q$    | $-7.67 \pm j1.60$   | $-1.04 \pm j5.96$   | $-0.030 \pm j2.89$ | $-0.63 \pm j0.84$   |                   |
|              | $H$ | $Z$    | $p, n$              | $0.0033 \pm j6.08$  | $-0.63 \pm j3.98$  | $-0.79 \pm j9.32$   | $-5.24 \pm j6.49$ |
|              |     | $P$    | $p$                 | $0.0033 \pm j0.20$  | $-0.63 \pm j2.30$  | $-0.79 \pm j3.03$   | $-5.24 \pm j0.20$ |
|              |     |        | $p$                 | $-0.80 \pm j9.15$   | $-6.46 \pm j6.04$  | $-6.36 \pm j0.10$   | $-1.21 \pm j3.17$ |
| $n$          |     |        | $-0.26 \pm j6.39$   | $-0.60 \pm j4.01$   | $-0.65 \pm j2.31$  | $0.0065 \pm j0.20$  |                   |
| $L_g=2.2$ mH | $Z$ | $d, q$ | $-0.0056 \pm j2.94$ | $-0.63 \pm j0.84$   | $-0.80 \pm j6.18$  | $-5.31 \pm j3.33$   |                   |
|              | $P$ | $d$    | $-0.91 \pm j6.48$   | $-5.30 \pm j3.33$   | $-0.22 \pm j3.33$  | $-0.62 \pm j0.86$   |                   |
|              |     | $q$    | $-7.67 \pm j1.59$   | $-1.04 \pm j5.97$   | $-0.037 \pm j2.90$ | $-0.63 \pm j0.84$   |                   |
|              | $H$ | $Z$    | $p, n$              | $-0.0056 \pm j6.10$ | $-0.63 \pm j3.98$  | $-0.80 \pm j9.32$   | $-5.31 \pm j6.48$ |
|              |     | $P$    | $p$                 | $-0.0056 \pm j0.19$ | $-0.63 \pm j2.30$  | $-0.80 \pm j3.04$   | $-5.31 \pm j0.19$ |
|              |     |        | $p$                 | $-0.81 \pm j9.16$   | $-6.50 \pm j6.02$  | $-6.40 \pm j0.13$   | $-1.21 \pm j3.17$ |
| $n$          |     |        | $-0.26 \pm j6.39$   | $-0.60 \pm j4.01$   | $-0.64 \pm j2.30$  | $-0.0028 \pm j0.19$ |                   |
| $L_g=2.1$ mH | $Z$ | $d, q$ | $-0.015 \pm j2.97$  | $-0.63 \pm j0.84$   | $-0.82 \pm j6.18$  | $-5.38 \pm j3.32$   |                   |
|              | $P$ | $d$    | $-0.92 \pm j6.48$   | $-5.38 \pm j3.33$   | $-0.22 \pm j3.33$  | $-0.62 \pm j0.86$   |                   |
|              |     | $q$    | $-7.67 \pm j1.58$   | $-1.04 \pm j5.98$   | $-0.045 \pm j2.92$ | $-0.63 \pm j0.84$   |                   |
|              | $H$ | $Z$    | $p, n$              | $-0.015 \pm j6.11$  | $-0.63 \pm j3.98$  | $-0.82 \pm j9.32$   | $-5.38 \pm j6.46$ |
|              |     | $P$    | $p$                 | $-0.015 \pm j0.17$  | $-0.63 \pm j2.30$  | $-0.82 \pm j3.04$   | $-5.38 \pm j0.17$ |
|              |     |        | $p$                 | $-0.82 \pm j9.18$   | $-6.54 \pm j6.00$  | $-6.45 \pm j0.16$   | $-1.20 \pm j3.17$ |
| $n$          |     |        | $-0.26 \pm j6.39$   | $-0.60 \pm j4.01$   | $-0.64 \pm j2.30$  | $-0.01 \pm j0.17$   |                   |

#### E. Comparative Study on Impedance-based Criteria for Overall Stability Analysis

The only reliable determinant-based criterion using the  $2 \times 2$  impedance matrix for the overall stability analysis is verified using Fig. 9. Considering the frame transformation, there is only a  $j\omega_0$  shift between  $\det(\mathbf{I}+R_{ZY}^{dq})$  and  $\det(\mathbf{I}+R_{ZY}^{pn})$ , hence the

former is plotted in Fig. 9 for simplicity and the origin should be  $(0,0j)$ . There are two clockwise encirclements around the origin when  $L_g$  is set as the maximum for both cases, hence the theoretical analysis using Fig. 8 matches simulations in Fig. 4. One should also note the locus is very concise with a stable open-loop system, which benefits the graphical analysis.

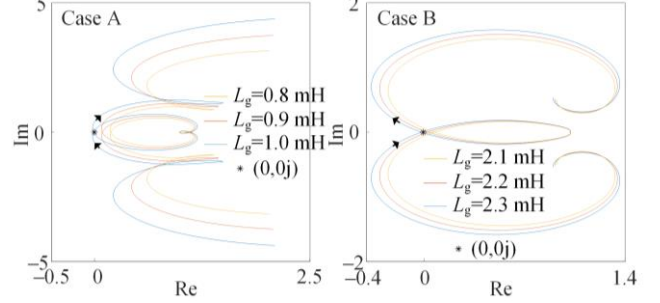


**Fig. 8.** Stability analysis using  $\det(\mathbf{I}+R_{ZY}^{dq})$ .

#### IV. LOGARITHMIC DERIVATIVE-BASED STABILITY CRITERION

##### A. Inspiration

Since this work calculates zeros and poles to support the distributed stability analysis, there is only one active-controlled AC loop in the studied system, and the conclusion of overall and distributed stability analyses should be equal. However, the distributed stability analysis is more of practical interest for positioning a critical loop and guiding a proper oscillation mitigating strategy design in the hybrid AC-DC systems, such as the back-to-back system studied in [20], where the detailed impedances of two AC loops and one DC loop are established. It is found that the overall instability can be identified by no more than two distributed stability analyses, hence tuning the control parameters which are closely related to the loop that cannot identify the stability should not be the first choice. In addition, there are some special cases where the aforementioned open-loop “no RHP pole” condition cannot be ensured, e.g., using a compensation device to stabilize an oscillating system, which even brings challenges to the reliable overall analysis in Section III.

Considering that for a loop impedance, the numerator can truthfully reflect partial system modes as (9) indicates while the uncertainty of positive real part roots for the denominator should be excluded in the stability criterion, a novel criterion based on the system mode identification is proposed as below.

##### B. Basic Principle

The targeted  $S_z$  can be written in a factored zero-pole form:

$$S_z(j\omega) = \prod_{i=1}^{n_z} a_{z_i}(j\omega - Z_i) / \prod_{i=1}^{n_p} a_{p_i}(j\omega - P_i) \quad (13)$$

where  $a$ ,  $n$ ,  $Z$ , and  $P$  (as well as the subscript) represent the flat gain, the order of polynomials, zeros, and poles, respectively.

Since the essential scope of stability analysis is to identify whether a positive real part  $Z_i$  exists in  $S_z$ , the basic unit for the numerator, i.e., a first-order polynomial  $g_z(\omega) = a_z(j\omega - \lambda_z)$ ,  $\lambda_z = \alpha_z + j\omega_z$ , is focused on. Recalling that the criterion in [19] regards the rest of  $S_z$  except  $g_z$  as a whole, requires the complex square root operations and the irrational

approximations, the *logarithmic derivative* on  $g_z$  can eliminate the effect of  $a_z$  and equalize each basic unit:

$$\begin{aligned} D_L(g_z) &= d \log(g_z) / d\omega = d(g_z) / (g_z d\omega) \\ &= j / (j\omega - \lambda_z) = j / [-\alpha_z + j(\omega - \omega_z)] \end{aligned} \quad (14)$$

The real-imaginary separation projects a complex output of  $D_L(g_z)$  to two real outputs for quantitative analyses:

$$\begin{cases} \text{Re}[D_L(g_z)] = (\omega - \omega_z) / [(\omega - \omega_z)^2 + \alpha_z^2] \\ \text{Im}[D_L(g_z)] = -\alpha_z / [(\omega - \omega_z)^2 + \alpha_z^2] \end{cases} \quad (15)$$

$$\Rightarrow \text{Re}[D_L(g_z)]|_{\omega=\omega_z} = 0, \quad \text{Im}[D_L(g_z)]|_{\omega=\omega_z} = -1 / \alpha_z.$$

Eq. (15) shows that a zero-crossing point exists for  $\text{Re}[D_L(g_z)]$  at  $\omega = \omega_z$ . To gain insights on  $\omega = \omega_z$ , the first and second derivatives of  $\text{Re}[D_L(g_z)]$  and  $\text{Im}[D_L(g_z)]$  are deduced:

$$\begin{cases} \frac{d\{\text{Re}[D_L(g_z)]\}}{d\omega} = \frac{-(\omega - \omega_z)^2 + \alpha_z^2}{[(\omega - \omega_z)^2 + \alpha_z^2]^2} \\ \frac{d\{\text{Im}[D_L(g_z)]\}}{d\omega} = \frac{-2(\omega - \omega_z)\alpha_z}{[(\omega - \omega_z)^2 + \alpha_z^2]^2} \end{cases}$$

$$\Rightarrow d\{\text{Re}[D_L(g_z)]\} / d\omega|_{\omega=\omega_z} = 1 / \alpha_z^2, \quad d\{\text{Im}[D_L(g_z)]\} / d\omega|_{\omega=\omega_z} = 0, \quad (16)$$

$$\begin{cases} \frac{d^2\{\text{Re}[D_L(g_z)]\}}{d\omega^2} = \frac{-2(\omega - \omega_z)[3\alpha_z^2 - (\omega - \omega_z)^2]}{[(\omega - \omega_z)^2 + \alpha_z^2]^3} \\ \frac{d^2\{\text{Im}[D_L(g_z)]\}}{d\omega^2} = \frac{-6(\omega - \omega_z)^2\alpha_z^2 + 2\alpha_z^3}{[(\omega - \omega_z)^2 + \alpha_z^2]^3} \end{cases}$$

$$\Rightarrow d^2\{\text{Re}[D_L(g_z)]\} / d\omega^2|_{\omega=\omega_z} = 0, \quad d^2\{\text{Im}[D_L(g_z)]\} / d\omega^2|_{\omega=\omega_z} = 2 / \alpha_z^3.$$

Therefore, when  $\alpha_z > 0$ , a negative minimum of  $\text{Im}[D_L(g_z)]$  and a positive slope of  $\text{Re}[D_L(g_z)]$  coexist at  $\omega = \omega_z$ , and a duality is satisfied for  $\text{Re}[D_L(1/g_z)]$  and  $\text{Im}[D_L(1/g_z)]$ , where  $(1/g_z)$  can be deemed as a basic unit of the denominator in  $S_z$ . The *frequency selectivity* induced by the inverse square term of  $\omega$  in (15) suppresses the interactions between zeros and poles, thus the weak negative damping mode can be identified quite exactly using (15) and (16). By substituting  $S_z$  into  $D_L(\cdot)$ , the process of applying the novel stability criterion is:

- 1) Obtaining the frequency responses of a dedicated  $S_z$ , by either adopting the frequency scans or performing the theoretical deductions based on (9).
- 2) Calculating the logarithmic derivative of frequency responses using the *difference method* and the first line in (14) with a small enough step such as 0.01Hz.
- 3) The system is determined as unstable when a minimum of  $\text{Im}[D_L(g_z)]$  and a positive slope of  $\text{Re}[D_L(g_z)]$  coexist at the same frequency ( $\omega = \omega_z$ ), and  $\alpha_z$  is calculated using the output of  $\text{Im}\{D_L[g_z(\omega_z)]\}$  and (15).

Since  $S_z$  is a general transfer function that contains the stability information of a closed-loop system, basic ideas of the proposed criterion can be extended to any other transfer-function-based analysis as long as one can find a proper transfer function, e.g.,  $u_{dc}^*(s)/u_{dc}(s)$  which uses the feedback and reference as output and input, respectively. More importantly, the proposed criterion can be applied without the “no RHP pole” condition, but plenty of transfer functions should be selected to ensure the observability to complete closed-loop system modes, and it is reasonable to select based on the number of physical loops since voltage and current are basic control objectives of power conversion.

## B. Validation

The stability assessments of Case A are illustrated in Fig. 9 for example. It can be observed that the magnitude of each  $S_z$  owns a pair of nadirs that are symmetrical about the central frequency (0 Hz for the sequence domain, 50 Hz for the  $dq$  domain, and the peaks/nadirs at  $\pm 50$  Hz in Fig. 9 (b) and 9 (c) are due to the calculation errors of the difference method and thus neglected). Consequently, it is more credible that using the various  $S_z$ s of the same AC loop but in various domains can achieve the same stability identification rather than the inconsistent feature of loci using unreliable impedance-based criteria shown in Fig. 5 and 7, which is similar to the feature of the determinant-based criterion shown in Fig. 8.

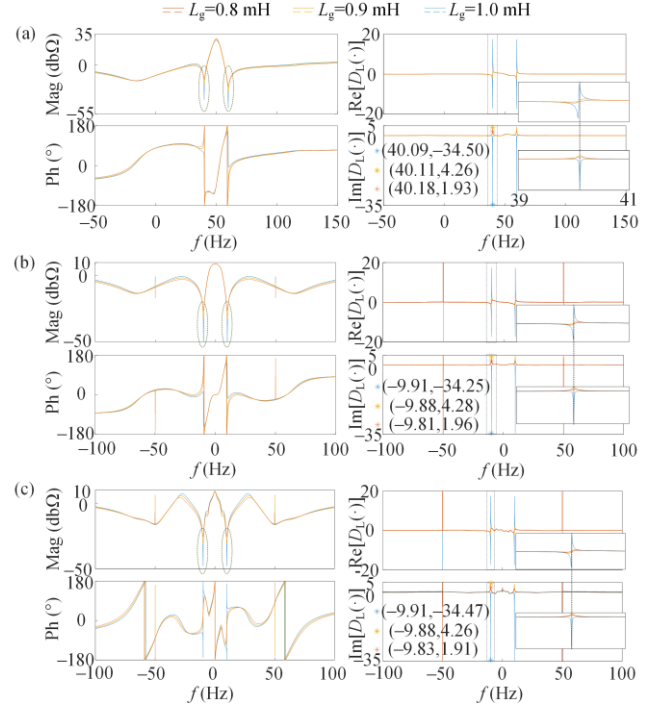


**Fig. 9.** Impedance characteristics of  $S_z$  with real-imaginary separations of  $D_L(S_z)$ . (a)  $p$ . (b)  $d$ . (c)  $q$ .

The logarithmic derivatives and real-imaginary separations are then performed on each  $S_z$ . It is found that the aforementioned nadirs lead to the zero-crossing points of  $\text{Re}[D_L(S_z)]$  with definite positive slopes when  $L_g$  varies, which means a zero of each  $S_z$  exists over a certain frequency range. Minimums for the case of  $L_g = 1$  mH and maximums for the case of  $L_g = 0.9$  &  $0.8$  mH are observed in the waveform of  $\text{Im}[D_L(S_z)]$ , and the value of extremes are very close for the models of both domains, thus the system is identified as unstable only when  $L_g = 1.0$  mH no matter which  $S_z$  is selected. In addition,  $\alpha_z$  is estimated as 0.1821,  $-1.4749$ , and  $-3.2555$  by dividing each extreme value by  $2\pi$  (note that the x-axis represents  $f$  instead of  $\omega$  in Fig. 9) in the sequence domain, and the results match the theoretical calculation in Table II and the simulated divergence rate of  $u_{dc}$  in Fig. 4; hence, the unstable mode can be estimated accurately enough. Even if the attribute of frequency selectivity will be influenced when the real parts of a pair of zero-pole are very close, the idea of

using the vector fitting or the unconstrained optimization to solve for the undetermined coefficients in the determined form based on (15) can be achieved, and the potential of assessing the system stability over a specific frequency range can be achieved using the proposed criterion.

## V. DISCUSSION AND CONCLUSION

### A. Overall Stability Analysis Using Transfer Immittances

The concept of transfer immittance is mentioned in Section II. B. Here more comments are offered to help readers correctly regard and apply such a scalable model for system-level analyses. Unlike a  $2 \times 2$  impedance/admittance matrix where only the dynamics on AC side are selected as the input/output of the open-loop system, the dynamic of DC side (with a superscript 0 below) is added as an element of the input/output vector which yields the  $3 \times 3$  transfer immittances for a TL-VSC [21]-[23]. [23] states that the input vector of the primary form of transfer immittances should be different when the TL-VSC is under the DC voltage control mode or the power control mode:

$$\begin{aligned} \text{Power control mode: } \begin{bmatrix} \Delta i^1 \\ \Delta i^2 \\ \Delta i^0 \end{bmatrix} &= \begin{bmatrix} Y^{11} & Y^{12} & Y^{13} \\ Y^{21} & Y^{22} & Y^{23} \\ Y^{31} & Y^{32} & Y^{33} \end{bmatrix} \begin{bmatrix} \Delta v^1 \\ \Delta v^2 \\ \Delta v^0 \end{bmatrix} \\ \text{DC voltage control mode: } \begin{bmatrix} \Delta i^1 \\ \Delta i^2 \\ \Delta v^0 \end{bmatrix} &= \begin{bmatrix} Y^{11} & Y^{12} & W^{13} \\ Y^{21} & Y^{22} & W^{23} \\ V^{31} & V^{32} & Z^{33} \end{bmatrix} \begin{bmatrix} \Delta v^1 \\ \Delta v^2 \\ \Delta i^0 \end{bmatrix} \end{aligned} \quad (17)$$

It is noticeable that the elements of the third column and row in the transfer immittance for the DC voltage control do not hold the unit of  $\Omega^{-1}$ , which is the real meaning of “immittance” instead of the notation in [21] where “immittance” is only used to contain the impedance and admittance. But [23] does not explain the reason to distinguish the transfer immittances under various control modes even if the conclusion is right. From the viewpoint of using the state space to obtain an arbitrary transfer function matrix that is introduced in Section III. B, it is found that  $\Delta v_0$  is a state variable and also the output variable for the DC voltage control mode, but can only be selected as an input variable for the power control mode. In other words, the two matrices in (17) satisfy the do not have RHP pole when a TL-VSC can stably operate fed by ideal sources, and the denominator of each element in (17) is equal to that in (4). By constructing the  $6 \times 6$  block matrices for both the equivalent converter- and grid-side, the determinant-based impedance criterion can be performed to analyze the overall stability reliably similar to Fig. 8, which is regarded as the correct application of transfer immittance instead of the application in [21] (See Appendix for the extension of such a modeling idea in a DC system). One can also establish the transfer immittance for the grid-forming converter or the grid-following converter under AC voltage control mode (the conclusion in [22] is questionable since the AC voltage (amplitude) control should not affect the input/output vectors in (17)), and should always give priority to the physical attribute of *voltage source converter* instead of a specific control mode for a proper model.

### B. Distributed Stability Analysis by Determinant Decomposing

The significance of distributed stability analysis is revealed in Section IV. A. Recent work [22] focuses on a 4-terminal DC grid which tries to achieve such a goal by decomposing the system determinant into 5 parts: One part is set to locate the instability at the DC sides with AC side dynamics included, which is similar with the loop impedance; the other four parts locate instability at each AC side but without DC side or the other AC dynamics included, which cannot identify the root cause (See (9), even if the authentic system modes can be reflected in the loop impedance, the lower right element only reflect the attribute of the open-loop system and surely does not reflect any closed-loop system modes; it is the RHP pole of loop impedance and the RHP zero of the open-loop impedance matrix together result in the questionable root cause identification of [22]). Hence, a mathematical determinant decomposing does not yield a successful distributed analysis.

Here a revised root cause identification is recommended:

- 1) Determining the number of physical (AC and DC) loops ( $N$ ) for an interconnected system.
- 2) Constructing the block-like transfer immittance sum matrix.
- 3) Applying the complete process of novel stability criterion of Section IV. B for the  $N$  loop in turn, by either changing the modeling domain (for AC loop) or changing the order of submatrix (for both AC and DC loop); once an RHP zero is identified, the loop can be regarded as one root cause of instability.
- 4) Counting the loops which identify unstable modes to guide the oscillation mitigation design.

The core idea of the revised identification is the proposed derivative-based stability criterion with more detailed considerations: On one hand, the Schur complement is performed separately for each physical loop, which ensures that the identified RHP zero is the authentic system mode; On the other hand, comparative studies are recommended as Fig. 9 indicates to exclude the *minimal possibility of zero-pole cancellation* due to the potentially emerged RHP pole of loop impedance as (9) indicates. In addition, a more reliable distributed analysis can also avoid the possible failure of the determinant-based criterion in identifying the special cases that are mentioned in Section IV.

### C. Revisiting Ref. [12]

It is widely recognized that [12] initiates the preference for performing the impedance-based method in converter-based AC systems over the recent 10 years. [12] majorly clarifies a practical condition of using Nyquist criteria in the power electronics field with the cooperated converter design guideline to ensure such a condition. Since frame coupling is not considered in [12], the obtained criterion for AC systems does not distinguish themselves from those for DC systems [1]. The theoretical foundation in Section II of this work proves that the idea in [12] is valuable and the most appealing point for the practical application of impedance-based

> REPLACE THIS LINE WITH YOUR MANUSCRIPT ID NUMBER (DOUBLE-CLICK HERE TO EDIT) <

methods, especially for the determinant-based criterion for the overall stability analysis as (5) indicates.

Unfortunately, lots of so-called “improved impedance-based criteria” (e.g., [16], [22]) obsess with the mathematical equivalence but dismiss the origin of the impedance-based method, especially for the distributed analysis, which stimulates this work. The particularity of the distributed stability analysis of Case A as shown in Fig. 5 should not be rare based on the simple explanation using (8) and Fig. 6, but it seems that no existing research specifically discusses such an observation (or one may just seek an alternative to avoid the special case). One should also realize since frequency responses are mostly available, ensuring the open-loop system without an RHP pole is much easier than counting the RHP pole of a transfer function functions, and the proposed revised criterion is expected to fully avoid the ambiguity induced by the RHP pole, which requires more specific implementations in the future.

#### D. Conclusion

Finally, the contributions of this work are reviewed. It is emphasized that the success of determinant-based overall stability analysis is ensured by the “no RHP condition” of the open-loop system, which is transformed to guarantee the stable operation of the converter- and grid-side subsystems and use the primary form of each transfer function matrix to form impedance ratio. Such a critical condition cannot adapt to the existing impedance-based criteria for distributed stability analyses, which is revealed using both theoretical deductions and Nyquist plots of a special case. A logarithmic derivative-based criterion with only the frequency responses of loop impedance as the input is proposed to serve as a useful tool for the unstable mode identification, which excludes the influence of RHP poles on the graphical stability analyses using Nyquist plots and makes it possible to let the distributed analysis “cover” the overall analysis. It is expected that several findings can guide future device-level modeling and system-level analysis, which are also separately discussed.

#### APPENDIX

Please find in arxiv.....

#### REFERENCES

- [1] R. D. Middlebrook, “Input filter considerations in design and application of switching regulators,” in *Proc. IEEE IAS Annu. Meeting*, Chicago, IL, USA, 1976, pp. 366–382.
- [2] A. Riccobono and E. Santi, “Comprehensive review of stability criteria for DC power distribution systems,” *IEEE Trans. Ind. Appl.*, vol. 50, no. 5, pp. 3525–3535, Sept.–Oct. 2014.
- [3] Technical Specification for Assessment of Impedance Characteristics of Wind Farm, NB/T 10651—2021, 2021.
- [4] M. Amin, C. Zhang, A. Rygg, M. Molinas, E. Unamuno, and M. Belkhaty, “Nyquist stability criterion and its application to power electronics systems” in *Wiley Encyclopedia of Electrical and Electronics Engineering*. Hoboken, NJ, USA: Wiley, 2019.
- [5] A. G. J. MacFarlane and H. Nyquist, *Frequency-Response Methods in Control Systems*. New York, NY, USA: IEEE Comput. Soc. Press, 1979.
- [6] C. Desoer and Y.-T. Wang, “On the generalized Nyquist stability criterion,” *IEEE Trans. Autom. Control*, vol. 25, no. 2, pp. 187–196, Apr. 1980.
- [7] L. Fan and Z. Miao, “Admittance-based stability analysis: bode plots, Nyquist diagrams or eigenvalue analysis?” *IEEE Trans. Power Syst.*, vol. 35, no. 4, pp. 3312–3315, July 2020.
- [8] S. Shah and L. Parsa, “Impedance modeling of three-phase voltage source converters in dq, sequence, and phasor domains,” *IEEE Trans. Energy Convers.* vol. 32, no. 3, pp. 1139–1150, Sept. 2017.
- [9] M. Kazem Bakhshizadeh et al., “Couplings in phase domain impedance modeling of grid-connected converters,” *IEEE Trans. Power Electron.*, vol. 31, no. 10, pp. 6792–6796, Oct. 2016.
- [10] M. Belkhaty, “Stability criteria for AC power systems with regulated loads,” Ph.D. dissertation, Purdue University, Washington, DC, 1997.
- [11] J. Sun, “Small-signal methods for AC distributed power systems—A review,” *IEEE Trans. Power Electron.*, vol. 24, no. 11, pp. 2545–2554, Nov. 2009.
- [12] J. Sun, “Impedance-based stability criterion for grid-connected inverters,” *IEEE Trans. Power Electron.*, vol. 26, no. 11, pp. 3075–3078, Nov. 2011.
- [13] Q.-C. Zhong and X. Zhang, “Impedance-sum stability criterion for power electronic systems with two converters/sources,” *IEEE Access*, vol. 7, pp. 21254–21265, 2019.
- [14] J. M. Maciejowski, *Multivariable Feedback Design*. Reading, MA, USA: Addison-Wesley, 1989.
- [15] J. Sun, “Frequency-domain stability criteria for converter-based power systems,” *IEEE Open J. Power Electron.*, vol. 3, pp. 222–254, 2022.
- [16] C. Zhang, X. Cai, A. Rygg, and M. Molinas, “Sequence domain SISO equivalent models of a grid-tied voltage source converter system for small-signal stability analysis,” *IEEE Trans. Energy Convers.*, vol. 33, no. 2, pp. 741–749, Jun. 2018.
- [17] Y. Liao and X. Wang, “Impedance-based stability analysis for interconnected converter systems with open-loop RHP poles,” *IEEE Trans. Power Electron.*, vol. 35, no. 4, pp. 4388–4397, Apr. 2020.
- [18] B. Gustavsen and A. Semlyen, “Rational approximation of frequency domain responses by vector fitting,” *IEEE Trans. Power Deliv.*, vol. 14, no. 3, pp. 1052–1061, Jul. 1999.
- [19] H. Liu, X. Xie, and W. Liu, “An oscillatory stability criterion based on the unified dq-frame impedance network model for power systems with high-penetration renewables,” *IEEE Trans. Power Syst.*, vol. 33, no. 3, pp. 3472–3485, May 2018.
- [20] C. Zhao and Q. Jiang, “Impedance-based AC/DC terminal modeling and analysis of MMC-BTB system,” *arXiv preprint arXiv:2206.12545*, 2022.
- [21] J. Sun, “Two-port characterization and transfer immittances of ac-dc Converters—Part I: Modeling,” *IEEE Open J. Power Electron.*, vol. 2, pp. 440–462, Aug. 2021.
- [22] H. Zhang, M. Saeedifard, X. Wang, Y. Meng, and X. Wang, “System harmonic stability analysis of grid-tied interlinking converters operating under AC voltage control mode,” *IEEE Trans. Power Syst.*, vol. 37, no. 5, pp. 4106–4109.
- [23] H. Zhang, X. Wang, M. Mehrbankhomartash, M. Saeedifard, Y. Meng, and X. Wang, “Harmonic stability assessment of multiterminal DC (MTDC) systems based on the hybrid AC/DC admittance model and determinant-based GNC,” *IEEE Trans. Power Electron.*, vol. 37, no. 2, pp. 1653–1665, Feb. 2022.
- [24] X. Wang, L. Harnefors, and F. Blaabjerg, “Unified impedance model of grid-connected voltage-source converters,” *IEEE Trans. Power Electron.*, vol. 33, no. 2, pp. 1775–1787, Feb. 2018.
- [25] B. Wen, D. Boroyevich, R. Burgos, P. Mattavelli, and Z. Shen, “Analysis of D-Q Small-Signal Impedance of Grid-Tied Inverters,” *IEEE Trans. Power Electron.*, vol. 31, no. 1, pp. 675–687, Jan. 2016.
- [26] M. Cespedes and J. Sun, “Impedance modeling and analysis of grid-connected voltage-source converters,” *IEEE Trans. Power Electron.*, vol. 29, no. 3, pp. 1254–1261, Mar. 2014.
- [27] Z. Xu, B. Li, S. Li, X. Wang, and D. Xu, “MMC admittance model simplification based on signal-flow graph,” *IEEE Trans. Power Electron.*, vol. 37, no. 5, pp. 5547–5561, May 2022.
- [28] S. Shah, P. Koralewicz, V. Gevorgian, and L. Parsa, “Small-signal modeling and design of phase-locked loops using harmonic signal-flow graphs,” *IEEE Trans. Energy Convers.*, vol. 35, no. 2, pp. 600–610, June 2020.
- [29] D. Yang and X. Wang, “Unified modular state-space modeling of grid-connected voltage-source converters,” *IEEE Trans. Power Electron.*, vol. 35, no. 9, pp. 9700–9715, Sep. 2020.
- [30] L. Fan, Z. Miao, and Z. Wang, “A new type of weak grid IBR oscillations,” *IEEE Trans. Power Syst.*, vol. 38, no. 1, pp. 988–991, Jan. 2023.

## APPENDIX

Fig. 10 reveals a basic topology of point-to-point DC transmission which realizes AC-DC-AC power conversion. If the DC cable is removed, it can be regarded as a back-to-back DC transmission that helps interconnect two AC grids. Here the DC stability is specially focused to emphasize the practical impedance-based criteria and AC impedances are neglected.

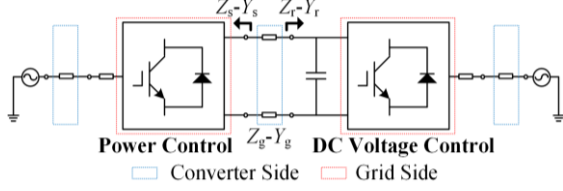


**Fig. 10.** Topology of point-to-point DC transmission.

For the back-to-back transmission ( $Z_g=0$ ), the well-recognized transfer function for DC stability analysis is  $(1+Z_r Y_s)$ , which indicates that if two converters can stably operate under ideal DC voltage (Power control mode) and current (DC voltage control mode) sources,  $Z_r Y_s$  does not have and one can draw the Nyquist plots to fast determine the system stability. While when using transfer functions such as  $(1+Z_s Y_r)$ ,  $(Z_s+Z_r)$ , or  $(Y_s+Y_r)$ , the RHP pole check is unavoidable theoretically before using the corresponding Nyquist plots to correctly identify the system stability. One can find help through the following equations when concluding the above observations into the impedance-based overall and distributed stability analysis framework discussed in this paper (the symbol ( $s$ ) is neglected for each element of the transfer function matrix):

$$\begin{aligned} \begin{bmatrix} v_r \\ i_s \end{bmatrix} &= \underbrace{\begin{bmatrix} Z_r & 0 \\ 0 & Y_s \end{bmatrix}}_{Z_{con}} \begin{bmatrix} i_r \\ v_s \end{bmatrix}, \quad \begin{bmatrix} i_r \\ v_s \end{bmatrix} = \underbrace{\begin{bmatrix} 0 & -1 \\ 1 & 0 \end{bmatrix}}_{Y_g} \begin{bmatrix} v_r \\ i_s \end{bmatrix}, \\ \text{Overall: } \det(1 + Z_{con} Y_g) &= \det(1 + Z_r Y_s) = 1 + Z_r Y_s. \\ \text{Distributed: } Z_{con} + Y_g^{-1} &= \begin{bmatrix} Z_r & 1 \\ -1 & Y_s \end{bmatrix}, \\ \det(Z_{con} + Y_g^{-1}) &= \det(\underbrace{Z_r + Z_s}_{\text{Loop Impedance 1}}) \times \det(Y_s) \\ &= \det(\underbrace{Y_r + Y_s}_{\text{Loop Impedance 2}}) \times \det(Z_r) \end{aligned} \quad (18)$$

It is intuitive that both the overall and distributed stability analyses can reflect the system mode but cannot embody the advantage of modular analysis using transfer immittances (which are simplified to DC impedances due to the fix of AC dynamics) over the direct analysis using DC impedances. However, when the case turns to the point-to-point transmission ( $Z_g \neq 0$ ), it seems like the partition point for correctly adopting the DC impedance-based analysis should be calibrated, and a reliable transfer function should be  $[1+(Z_g+Z_r)Y_s]$ , whose explanations using transfer immittances are listed as below:

$$\begin{aligned} \begin{bmatrix} v_r \\ i_s \end{bmatrix} &= \underbrace{\begin{bmatrix} Z_r & 0 \\ 0 & Y_s \end{bmatrix}}_{Z_{con}} \begin{bmatrix} i_r \\ v_s \end{bmatrix}, \quad \begin{bmatrix} i_r \\ v_s \end{bmatrix} = \underbrace{\begin{bmatrix} 0 & -1 \\ 1 & Z_g \end{bmatrix}}_{Y_g} \begin{bmatrix} v_r \\ i_s \end{bmatrix}, \\ \text{Overall: } \det(1 + Z_{con} Y_g) &= \det\left(\begin{bmatrix} 1 & -Z_r \\ Y_s & 1 + Y_s Z_g \end{bmatrix}\right) = 1 + Y_s (Z_g + Z_r). \\ \text{Distributed: } Z_{con} + Y_g^{-1} &= \begin{bmatrix} Z_r + Z_g & 1 \\ -1 & Y_s \end{bmatrix}, \\ \det(Z_{con} + Y_g^{-1}) &= \det(\underbrace{Z_r + Z_g + Z_s}_{\text{Loop Impedance 1}}) \times \det(Y_s) \\ &= \det(\underbrace{Y_s + (Z_r + Z_g)^{-1}}_{\text{Loop Impedance 2}}) \times \det(Z_r + Z_g) \end{aligned} \quad (19)$$

Eq. (19) confirms the reliability of the determinant-based criterion when formulating the transfer immittance to a right pattern without an RHP pole, and from the viewpoint of DC impedance analysis, there is no essential difference between the cases of aggregating the DC cable to either converter, but to assess the number of RHP pole is very important (i.e., one cannot say a criterion using  $(Z_s+Z_r+Z_g)$  or  $[Y_s+(Z_r+Z_g)^{-1}]$  is wrong). One can also compare the overall stability analysis between using transfer immittance in (19) with the idea of using node admittance/impedance:

$$\begin{aligned} \begin{bmatrix} v_r \\ v_s \end{bmatrix} &= \underbrace{\begin{bmatrix} Z_r & 0 \\ 0 & Z_s \end{bmatrix}}_{Z_{con}} \begin{bmatrix} i_r \\ i_s \end{bmatrix}, \quad \begin{bmatrix} i_r \\ i_s \end{bmatrix} = \underbrace{\begin{bmatrix} Y_g & -Y_g \\ -Y_g & Y_g \end{bmatrix}}_{Y_g} \begin{bmatrix} v_r \\ v_s \end{bmatrix}, \\ \text{Overall: } \det(1 + Z_{con} Y_g) &= \det\left(\begin{bmatrix} 1 + Z_r Y_g & -Z_r Y_g \\ -Z_s Y_g & 1 + Z_s Y_g \end{bmatrix}\right) = 1 + Y_g (Z_s + Z_r). \end{aligned} \quad (20)$$

It can be found in (20) that due to the uncertain RHP pole distribution of  $Z_s$ , the reliability of overall stability analysis without RHP pole check is destroyed, which breaks the major advantage of impedance-based analysis. Such an intuitive observation indicates the necessity of using Eq. (17) for a hybrid AC-DC system. An extra comment is that when one tries to develop an analytical transfer immittance using harmonic linearization, it may not be straightforward to formulate the input/output vector as listed in (17), especially for modular multilevel converters, and the techniques of reformulating the transfer immittance can be realized combining with the Schur complement as introduced in Eq. (9).